

UCD-94-6  
NUHEP-TH-94-2  
March 1994

## SEARCH FOR ANOMALOUS COUPLINGS AT $e\gamma$ COLLIDERS

**Kingman Cheung,<sup>(a)</sup> S. Dawson,<sup>(b)</sup> T. Han,<sup>(c)</sup> and G. Valencia<sup>(d)</sup>**

<sup>(a)</sup> *Department of Physics, Northwestern University, Evanston, IL 60208*

<sup>(b)</sup> *Physics Department, Brookhaven National Laboratory, Upton, NY 11973*

<sup>(c)</sup> *Department of Physics, University of California at Davis, Davis CA 95616*

<sup>(d)</sup> *Department of Physics, Iowa State University, Ames IA 50011*

### Abstract

We consider the possibility of observing deviations from the Standard Model gauge-boson self-couplings at future  $e\gamma$  colliders. We concentrate on the process  $e^-\gamma \rightarrow \nu W^- Z$ , which is particularly sensitive to the parity violating coupling  $g_5^Z$  at high energies. We find that a 2 TeV  $e^+e^-$  collider operating in the  $e^-\gamma$  mode could reach a sensitivity of order  $5 \times 10^{-3}$  to  $g_5^Z$ .

# 1 Introduction

The Standard Model of electroweak interactions (SM) has been tested thoroughly in many experiments. The only missing ingredients are the top-quark and the Higgs-boson. Whereas we expect that the top-quark will be found in the near future, the same cannot be said for the Higgs-boson. The Higgs-boson in the Standard Model is responsible for the breaking of electroweak symmetry, and experiments conducted thus far have not tested directly the energy scales at which the symmetry breaking is thought to occur.

There are many different physics possibilities that could be responsible for the breaking of the electroweak symmetry. On general grounds we expect that there will be new particles associated with the symmetry breaking sector, like the Higgs boson or whatever takes its place. The purpose of new high energy colliders is to explore the energy scales associated with the breaking of electroweak symmetry. However, it is possible that any given machine will be operating at energies below that which is necessary to excite the lightest new particle. In that case, we would like to study gauge boson interactions and try to infer from them what the new physics could be. This scenario makes it interesting to parameterize the symmetry breaking sector of the theory in a model independent way by means of an effective Lagrangian, and to explore the sensitivity of present and future experiments to the couplings introduced in this parameterization.

In this paper we will look at the capability of future  $e\gamma$  colliders to study the “anomalous” gauge boson couplings. Such colliders with high energy and high luminosity can potentially be made from  $e^+e^-$  linear colliders using the laser back-scattering method [1]. The possibility of observing the SM Higgs boson at such colliders through the process  $e^-\gamma \rightarrow \nu W^- H$  has been previously discussed, and it was found that a 1 TeV  $e^+e^-$  collider operating in the  $e\gamma$  mode should be able to discover a Higgs boson in the intermediate mass range 60 – 150 GeV [2, 3]. Here we assume that there is no Higgs boson (at least not with a mass that makes it directly accessible to the machine) and investigate the sensitivity of an  $e\gamma$  collider to the three and four gauge-boson self-interactions [4]. We concentrate on the process  $e^-\gamma \rightarrow \nu W^- Z$  for several reasons. This process depends on only a few of the anomalous couplings, and at very high energies it singles out one coupling. The process is thus ideally suited to isolate the effects of this one coupling, the parity violating but  $CP$  conserving  $g_5^Z$ . This process also has a relatively small SM background as we will discuss in section 3.

In Section 2, we summarize the effective Lagrangian formalism that we use to describe the “anomalous” couplings. We derive all the Feynman rules needed to compute the amplitude for  $e^-\gamma \rightarrow \nu W^- Z$ . In section 3 we present our numerical results and discuss the sensitivity of an  $e^-\gamma$  collider to the anomalous couplings. Finally, in section 4 we present our conclusions.

## 2 Anomalous Couplings

We start from the minimal effective Lagrangian that describes the interactions of gauge bosons of an  $SU(2)_L \times U(1)_Y$  gauge symmetry spontaneously broken to  $U(1)_Q$ . In this case the gauge boson mass and kinetic energy terms are [5]:

$$\mathcal{L}^{(2)} = \frac{v^2}{4} \text{Tr} \left( D^\mu \Sigma^\dagger D_\mu \Sigma \right) - \frac{1}{2} \text{Tr} \left( W^{\mu\nu} W_{\mu\nu} \right) - \frac{1}{2} \text{Tr} \left( B^{\mu\nu} B_{\mu\nu} \right) \quad , \quad (1)$$

where  $W_{\mu\nu}$  and  $B_{\mu\nu}$  are the  $SU(2)$  and  $U(1)$  field strength tensors given in terms of  $W_\mu \equiv W_\mu^i \tau_i$ , by:<sup>1</sup>

$$\begin{aligned} W_{\mu\nu} &= \frac{1}{2} \left( \partial_\mu W_\nu - \partial_\nu W_\mu + \frac{i}{2} g [W_\mu, W_\nu] \right) \\ B_{\mu\nu} &= \frac{1}{2} \left( \partial_\mu B_\nu - \partial_\nu B_\mu \right) \tau_3. \end{aligned} \quad (2)$$

The matrix  $\Sigma \equiv \exp(i\vec{\omega} \cdot \vec{\tau}/v)$ , contains the would-be Goldstone bosons  $\omega_i$  that give the  $W$  and  $Z$  their mass via the Higgs mechanism, and the  $SU(2)_L \times U(1)_Y$  covariant derivative is given by:

$$D_\mu \Sigma = \partial_\mu \Sigma + \frac{i}{2} g W_\mu^i \tau^i \Sigma - \frac{i}{2} g' B_\mu \Sigma \tau_3. \quad (3)$$

The first term in Eq. 1 is the  $SU(2)_L \times U(1)_Y$  gauge invariant mass term for the  $W$  and  $Z$ . The physical masses are obtained with  $v \approx 246$  GeV. This non-linear realization of the symmetry breaking sector contains the same low energy physics as the minimal Standard Model when the Higgs-boson is taken to be very heavy [5]. It is a non-renormalizable theory that is interpreted as an effective field theory, valid below some scale  $\Lambda \leq 3$  TeV. The lowest order interactions between the gauge bosons and fermions are the same as those in the minimal Standard Model.

In writing the Lagrangian of Eq. 1 we assumed a custodial  $SU(2)_C$  symmetry broken only by the hypercharge coupling  $g'$ . Without this assumption, there can be one more term in the lowest order effective Lagrangian:

$$\mathcal{L}^{(2)'} = \frac{1}{8} \Delta \rho v^2 \left[ \text{Tr} \left( \tau_3 \Sigma^\dagger D_\mu \Sigma \right) \right]^2. \quad (4)$$

This term describes deviations of the  $\rho$  parameter from one. Since, experimentally,  $\Delta \rho$  is very small:  $\Delta \rho = (1.5 \pm 2.6) \times 10^{-3}$  [6], we will neglect  $\mathcal{L}^{(2)'}$ .

The “anomalous” gauge boson couplings that we want to study correspond to other  $SU(2)_L \times U(1)_Y$  gauge invariant operators one can write besides those in Eq. 1. For “low energy” processes, those that occur at energies below the scale of symmetry breaking  $\Lambda$ , it is possible to organize the effective Lagrangian in a way corresponding to an expansion of high energy scattering amplitudes in powers of  $E^2/\Lambda^2$ . The next

---

<sup>1</sup> The Pauli matrices are normalized such that  $\text{Tr}(\tau_i \tau_j) = 2\delta_{ij}$ .

to leading order effective Lagrangian that arises in this context has been discussed at length in the literature [5, 7, 8, 9, 10].

We will consider the next-to-leading order effective Lagrangian containing all terms which conserve the custodial  $SU(2)_C$  (up to hypercharge couplings). In addition, we will consider a special operator which apart from breaking the custodial symmetry, violates parity and charge conjugation while conserving  $CP$  [11]. The process that we discuss in this paper,  $e^- \gamma \rightarrow \nu W^- Z$ , is sensitive to the  $\gamma ZWW$  interaction. At very high energies, the amplitude for the process  $\gamma W^- \rightarrow ZW^-$  is enhanced when the  $W^-$  and  $Z$  are longitudinally polarized. Roughly, the amplitude gains an enhancement factor  $\sqrt{s}/M_W$  for each longitudinal polarization, and the largest enhancement is thus obtained when all three gauge bosons are longitudinally polarized. We could compute this enhanced amplitude by using the equivalence theorem and replacing each longitudinally polarized gauge boson with its corresponding would-be Goldstone boson. For the largest enhancement we would thus be calculating the amplitude for  $\gamma \omega^- \rightarrow \omega^0 \omega^-$  ( $\omega^\pm, \omega^0$  are the would-be Goldstone bosons corresponding to the longitudinal components of the  $W$  and  $Z$ ). However, this process will not take place unless parity is violated (since we are not considering the possibility of having Wess-Zumino-Witten terms for the effective theory). This leads us to believe that the process  $e^- \gamma \rightarrow \nu W^- Z$  will single out the parity violating couplings at high energy. For this reason, out of the many terms that break the custodial symmetry in the next to leading order Lagrangian, we only consider the one that also violates parity. This term will yield enhanced interactions at high energies. There are other terms that violate parity, but they also violate  $CP$ . We know that the weak interactions violate parity maximally, but that observed  $CP$  violation is very small. With this in mind, we do not expect the  $P$  violating but  $CP$  conserving operator to have any special suppression factors in general. At the same time, we might expect the  $CP$  violating operators to have smaller couplings than one would estimate from simple power counting rules. We will not consider the  $CP$  violating operators in this paper.

We are thus left with the following next-to-leading order effective Lagrangian:

$$\begin{aligned} \mathcal{L}^{(4)} = & \frac{v^2}{\Lambda^2} \left\{ L_1 \left[ \text{Tr} \left( D^\mu \Sigma^\dagger D_\mu \Sigma \right) \right]^2 + L_2 \text{Tr} \left( D_\mu \Sigma^\dagger D_\nu \Sigma \right) \text{Tr} \left( D^\mu \Sigma^\dagger D^\nu \Sigma \right) \right. \\ & - ig L_{9L} \text{Tr} \left( W^{\mu\nu} D_\mu \Sigma D_\nu \Sigma^\dagger \right) - ig' L_{9R} \text{Tr} \left( B^{\mu\nu} D_\mu \Sigma^\dagger D_\nu \Sigma \right) \\ & \left. + gg' L_{10} \text{Tr} \left( \Sigma B^{\mu\nu} \Sigma^\dagger W_{\mu\nu} \right) + g\hat{\alpha} \epsilon^{\alpha\beta\mu\nu} \text{Tr} \left( \tau_3 \Sigma^\dagger D_\mu \Sigma \right) \text{Tr} \left( W_{\alpha\beta} D_\nu \Sigma \Sigma^\dagger \right) \right\}. \end{aligned} \quad (5)$$

The terms with the  $L_i$  are the five terms that conserve the custodial  $SU(2)_C$  symmetry. We explicitly introduce the factor  $v^2/\Lambda^2$  in our definition of  $\mathcal{L}^{(4)}$  so that the  $L_i$  are naturally of  $\mathcal{O}(1)$ . The term with  $\hat{\alpha}$  is the one that breaks custodial symmetry and violates parity while conserving  $CP$ . With the normalization we have given  $\mathcal{L}^{(4)}$ , we expect  $\hat{\alpha}$  to be of  $\mathcal{O}(1)$  in theories without a custodial symmetry and of order  $\Delta\rho$  in theories that have a custodial symmetry [11]. For our discussion we will assume that the new physics is such that the tree-level coefficients of  $\mathcal{L}^{(4)}$  are larger than the (formally of the same order) effects induced by  $\mathcal{L}^{(2)}$  at one-loop. More precisely,

that after using dimensional regularization and a renormalization scheme similar to the one we used in Ref. [8], the  $L_i(\mu)$  evaluated at a typical scale around  $\Lambda$  are equal to the tree-level coefficients and that the running is unimportant for the energies of interest. The physical motivation for this assumption is that, even if we do not see any new resonances directly, the effects of the new physics from high mass scales must clearly stand out if there is to be any hope of observing them. When the indirect effects of the new physics enter at the level of SM radiative corrections, very precise experiments (as the ones being performed at LEP I) are needed to unravel them. We are assuming that there will not be any such precision measurements in the next generation of high energy colliders.

We can find the Feynman rules by going to unitary gauge,  $\Sigma = 1$ , and expanding the Lagrangians of Eqs. 1 and 5. The operator in front of  $L_{10}$ , however, contributes terms bilinear in the gauge boson fields to the effective Lagrangian. It is therefore necessary to perform additional transformations on the fields  $A$  and  $Z$  that appear in our effective Lagrangian to obtain the physical fields. We follow Holdom [7], and use the “\*” renormalization scheme of Kennedy and Lynn [12] which is defined by the relation:

$$s_Z^2 c_Z^2 \equiv \frac{\pi \alpha^*}{\sqrt{2} G_F M_Z^{\text{phys}}}, \quad (6)$$

where  $s_Z$  ( $c_Z$ ) is the sine (cosine) of the weak mixing angle renormalized at the scale of  $M_Z$ ,  $s_Z = \sin \theta_W$ . We thus use as input parameters:  $G_F$  as measured in muon decay; the physical  $Z$  mass,  $M_Z^{\text{phys}} = 91.17$  GeV, and  $\alpha^* = 1/128.8$ . In terms of these quantities we thus use  $v = 1/\sqrt{\sqrt{2} G_F}$ .

Our next-to-leading order amplitudes will get direct contributions from the terms in  $\mathcal{L}^{(4)}$ , as well as contributions from the renormalization of  $\mathcal{L}^{(2)}$  (including the couplings to fermions that we have not written). To the order we are working, this renormalization is accomplished by replacing the unrenormalized quantities  $e$ ,  $c_\theta$ ,  $s_\theta$  and  $M_Z^0$  appearing in  $\mathcal{L}^{(2)}$  in the following way [7]:

$$\begin{aligned} c_\theta &= c_Z \left( 1 - \frac{2s_Z^2 e^{*2}}{s_Z^2 - c_Z^2} L_{10} \frac{v^2}{\Lambda^2} \right) \\ s_\theta &= s_Z \left( 1 + \frac{2c_Z^2 e^{*2}}{s_Z^2 - c_Z^2} L_{10} \frac{v^2}{\Lambda^2} \right) \\ M_Z^0 &= \left( 1 + e^{*2} L_{10} \frac{v^2}{\Lambda^2} \right) M_Z^{\text{phys}} \\ e &= \left( 1 - e^{*2} L_{10} \frac{v^2}{\Lambda^2} \right) e^*, \end{aligned} \quad (7)$$

and by re-writing the lowest order Lagrangian in terms of the physical fields. The only fields that change are those corresponding to the neutral gauge bosons:

$$\begin{aligned} Z &\rightarrow \left( 1 - e^{*2} L_{10} \frac{v^2}{\Lambda^2} \right) Z \\ A &\rightarrow \left( 1 + e^{*2} L_{10} \frac{v^2}{\Lambda^2} \right) A + \frac{(c_Z^2 - s_Z^2)}{s_Z c_Z} e^{*2} L_{10} \frac{v^2}{\Lambda^2} Z \quad . \end{aligned} \quad (8)$$

The relevant Feynman rules are given in the Appendix.

It has become conventional in the literature to parameterize the three gauge boson vertex  $VW^+W^-$  (where  $V = Z, \gamma$ ) in the following way [13]:

$$\begin{aligned}\mathcal{L}_{WWV} = & -ie_* \frac{c_Z}{s_Z} g_1^Z \left( W_{\mu\nu}^\dagger W^\mu - W_{\mu\nu} W^{\mu\dagger} \right) Z^\nu - ie_* g_1^\gamma \left( W_{\mu\nu}^\dagger W^\mu - W_{\mu\nu} W^{\mu\dagger} \right) A^\nu \\ & -ie_* \frac{c_Z}{s_Z} \kappa_Z W_\mu^\dagger W_\nu Z^{\mu\nu} - ie_* \kappa_\gamma W_\mu^\dagger W_\nu A^{\mu\nu} \\ & -e^* \frac{c_Z}{s_Z} g_5^Z \epsilon^{\alpha\beta\mu\nu} \left( W_\nu^- \partial_\alpha W_\beta^+ - W_\beta^+ \partial_\alpha W_\nu^- \right) Z_\mu \quad .\end{aligned}\tag{9}$$

For comparison with the literature we present our results in this form: <sup>2</sup>

$$\begin{aligned}g_1^Z &= 1 + \frac{e^2}{c_\theta^2} \left( \frac{1}{2s_\theta^2} L_{9L} + \frac{1}{(c_\theta^2 - s_\theta^2)} L_{10} \right) \frac{v^2}{\Lambda^2} \\ g_1^\gamma &= 1 \\ \kappa_Z &= 1 + e^2 \left( \frac{1}{2s_\theta^2 c_\theta^2} \left( L_{9L} c_\theta^2 - L_{9R} s_\theta^2 \right) + \frac{2}{(c_\theta^2 - s_\theta^2)} L_{10} \right) \frac{v^2}{\Lambda^2} \\ \kappa_\gamma &= 1 + \frac{e^2}{s_\theta^2} \left( \frac{L_{9L} + L_{9R}}{2} - L_{10} \right) \frac{v^2}{\Lambda^2} \\ g_5^Z &= \frac{e^2}{s_\theta^2 c_\theta^2} \hat{\alpha} \frac{v^2}{\Lambda^2}.\end{aligned}\tag{10}$$

The difference between  $e$  and  $e^*$ ,  $s_\theta$  and  $s_Z$  in Eq. 10 is higher order and can be neglected.

The four gauge boson interaction is derived from Eqs. 1 and 5 and can be written as:

$$\begin{aligned}\mathcal{L}_{WWZA} = & -e^{*2} \frac{c_Z}{s_Z} g_1^Z \left( 2W^+ \cdot W^- A \cdot Z - A \cdot W^+ Z \cdot W^- - Z \cdot W^+ A \cdot W^- \right) \\ & + i 2e^{*2} \frac{c_Z}{s_Z} g_5^Z \epsilon^{\alpha\beta\mu\nu} W_\alpha^- W_\beta^+ Z_\mu A_\nu\end{aligned}\tag{11}$$

It is important to see how, in a gauge invariant description of anomalous couplings, the coefficients of the three and four gauge boson couplings are related. Of course, the specific relation implicit in Eqs. 10 and 11 may change if other custodial  $SU(2)_C$  violating terms are included in the Effective Lagrangian.

Our effective Lagrangian formalism breaks down at some scale  $\Lambda \leq 3$  TeV, and this manifests itself in amplitudes that grow with energy and violate unitarity at some scale related to  $\Lambda$ . In order to stay within the region of validity of our description, we

---

<sup>2</sup>We agree with the results of Appelquist and Wu [10] when we make the identification,  $\alpha_1 = \frac{v^2}{\Lambda^2} L_{10}$ ,  $\alpha_2 = \frac{v^2}{\Lambda^2} \frac{L_{9R}}{2}$ ,  $\alpha_3 = \frac{v^2}{\Lambda^2} \frac{L_{9L}}{2}$ , and with those of Holdom [7] when we use  $L_9^{\text{Holdom}} = -\frac{v^2}{\Lambda^2} \frac{(L_{9L} + L_{9R})}{2}$ . The terms proportional to  $L_{9L}$  and  $L_{9R}$  agree with those of Boudjema [14]. However, there are several typos in the results of Falk, Luke, and Simmons [9].

compute the  $J = 0$  partial wave for different amplitudes and require that it be less than one. For the process  $\omega^- \gamma \rightarrow \omega^- \omega^0$ , we find:

$$|a_0|_{\pm} = \frac{1}{16\sqrt{2}} e^* \hat{\alpha} \frac{\sqrt{s_{\omega\gamma}}}{v} \frac{s_{\omega\gamma}}{\Lambda^2} \quad (12)$$

where  $\sqrt{s_{\omega\gamma}}$  denotes the center of mass energy of the  $\omega^- \gamma$  system. For example, if we are interested in studying this process at  $\sqrt{s_{\omega\gamma}} = 2$  TeV and we take the scale of new physics to be 2 TeV, the requirement that  $|a_0|_{\pm} \leq 1$  leads to the unitarity bound  $|\hat{\alpha}| \leq 9$ , or  $|g_5^Z| \leq 0.08$ . Notice, however, that this unitarity bound is less strict for processes at lower energies. This simply corresponds to the conventional wisdom that the physics associated with electroweak symmetry breaking must appear at (or below) a scale of a few TeV.

It turns out that the process  $\omega^- Z \rightarrow \omega^- \omega^0$ , provides a slightly tighter unitarity constraint on  $\hat{\alpha}$ , and it also allows us to compare it with unitarity bounds on other anomalous couplings. For example, the lowest order Lagrangian and the term with  $L_1$  in Eq. 5 also contribute to this process. If we again compute the helicity amplitudes for transverse  $Z$  polarizations and take the  $J = 0$  partial wave we find:

$$|a_0|_{\pm} = \frac{1}{128\sqrt{2}} \frac{e^*}{s_Z c_Z} \frac{\sqrt{s_{\omega Z}}}{v} \left( 1 + 4L_1 \frac{s_{\omega Z}}{\Lambda^2} + 8\hat{\alpha} c_Z^2 \frac{s_{\omega Z}}{\Lambda^2} \right). \quad (13)$$

If we look instead at the amplitude with a longitudinal  $Z$  we find:

$$|a_0|_L = \frac{1}{32\pi} \frac{s_{\omega Z}}{v^2} \left( 1 + \frac{16L_1}{3} \frac{s_{\omega Z}}{\Lambda^2} \right). \quad (14)$$

We now adopt the “naturalness” argument that each term should be independently smaller than the unitarity bound. Taking again  $\sqrt{s_{\omega Z}} = \Lambda = 2$  TeV we find from Eq. 13 the bounds  $|\hat{\alpha}| \leq 4.9$  and  $|L_1| \leq 7.6$ . We see that unitarity bounds for both couplings are of the same order. However, Eq. 14 places the much stronger bound  $|L_1| \leq 0.3$ .<sup>3</sup> This is well understood from the fact that at high energies one obtains larger amplitudes for longitudinally polarized gauge bosons. Since  $\hat{\alpha}$  does not contribute to  $\omega\omega$  scattering processes, the constraint on it from unitarity is weaker than that on its counterparts  $L_1$  and  $L_2$ . On the other hand,  $L_9$  and  $L_{10}$  will only contribute to four gauge boson scattering amplitudes when at least two of them are transversely polarized. This can be seen from the results we presented in Appendix A of Ref. [8]. One then finds that the unitarity bounds on  $L_9$  and  $L_{10}$  are very loose. For example, from  $VV \rightarrow \omega\omega$  processes with  $\sqrt{s_{VV}} = \Lambda = 2$  TeV, they are of the order of  $L_{9L,9R,10} \leq 500$ . Bounds on these couplings from unitarity of  $q\bar{q} \rightarrow \omega\omega$  processes are even weaker.

### 3 Phenomenological Studies for $e^- \gamma \rightarrow \nu W^- Z$

In this section we consider the phenomenology of the process  $e^- \gamma \rightarrow \nu W^- Z$  as it could be studied in future  $e^+e^-$  or  $e^-e^-$  colliders operating in the  $e\gamma$  mode. Within the

---

<sup>3</sup>This is consistent with the results of a more general analysis shown in figure 1 of Ref. [8]

SM, this process has been considered in Ref. [2]. The diagrams needed to compute the amplitude are shown in Figure 1. We evaluate these amplitudes numerically using helicity amplitude techniques. We have also checked the electromagnetic gauge invariance numerically. This check is done separately for the amplitude corresponding to each operator since they all must be separately gauge invariant.

We find that the new interactions proportional to  $L_1$  and  $L_2$  do not contribute to this process. The new interactions proportional to  $\hat{\alpha}$ ,  $L_{9L}$ ,  $L_{9R}$ , and  $L_{10}$  contribute not only to the gauge-boson fusion diagrams, but to all other diagrams as well. This is shown in Figure 1. The shaded circles on vertices indicate modifications induced by the new couplings. This interplay of different couplings induced by the same gauge invariant operator makes the importance of our effective Lagrangian formulation manifest.<sup>4</sup>

In Ref. [11], we computed the amplitude for  $e^-\gamma \rightarrow \nu W^- Z$  using the effective  $W$  approximation. The results indicated that at very high energies, this process is particularly sensitive to the  $\hat{\alpha}$  coupling. This is, of course, due to the enhanced couplings made possible by the parity violating nature of this operator. In this section we compute the amplitude exactly in order to obtain more quantitative results.

We present all of our numerical results for  $e^+e^-$  colliders. This involves folding the  $e^-\gamma \rightarrow \nu W^- Z$  differential cross-sections with the energy spectrum of the backscattered photon. The cross section for  $e^+e^- \rightarrow e^+\nu W^- Z$  is then,

$$\sigma(s_{ee}) = \int_{x_{\min}}^{x_{\max}} dx F_{\gamma/e}(x) \hat{\sigma}_{e\gamma}(xs_{ee}), \quad (15)$$

where  $s_{ee}$  the squared center of mass energy of the  $e^+e^-$  system. The unpolarized photon luminosity is given by [1]:

$$F_{\gamma/e}(x) = \frac{1}{D(\zeta)} \left( 1 - x + \frac{1}{1-x} - \frac{4x}{\zeta(1-x)} + \frac{4x^2}{\zeta^2(1-x)^2} \right) \quad (16)$$

and

$$D(\zeta) = \left( 1 - \frac{4}{\zeta} - \frac{8}{\zeta^2} \right) \log(1+\zeta) + \frac{1}{2} + \frac{8}{\zeta} - \frac{1}{2(1+\zeta)^2} \quad (17)$$

The parameter  $\zeta$  is given by  $\zeta = 4E_0\omega_0/m_e^2$ , where  $\omega_0$  is the energy of the incoming laser photon and  $E_0$  is the  $e^-$  beam energy.  $x$  is the fraction of the electron energy carried by the backscattered photon,  $x_{\max} = \zeta/(1+\zeta)$ , and  $x_{\min}$  is determined by the kinematical limit  $(M_W + M_Z)^2/s_{ee}$ . The value for  $\zeta$  is chosen in such a way that the backscattered photon cannot interact with the incident photon to produce an unwanted  $e^+e^-$  pair. This requirement implies  $\omega_0 x_{\max} \leq m_e^2/E_0$  which gives  $\zeta \leq 4.8$ . We choose  $\zeta = 4.8$  to maximize  $x_{\max}$ , and this yields  $x_{\max} = 0.83$ ,  $D(\zeta) = 1.8$  and  $\omega_0 = 1.25$  eV for a 0.5 TeV  $e^+e^-$  collider.

In Fig. 2, we show the total cross section as a function of  $\sqrt{s_{ee}}$  for  $\Lambda = 2$  TeV. We have adopted the usual “naturalness” assumption, that the process can independently

---

<sup>4</sup>This process was recently considered by Eboli *et al.*[15]. That paper, however, does not use a consistent and gauge invariant formalism.



place bounds on the different anomalous couplings that contribute to it. This means that we only look at one anomalous coupling at a time and ignore possible interference between terms with different anomalous couplings. There are four curves in the plot: the solid one corresponds to the lowest order amplitude only (that arising from  $\mathcal{L}^{(2)}$ ); the dashed curve corresponds to the  $\mathcal{L}^{(2)}$  amplitude plus the one obtained from  $\mathcal{L}^{(4)}$  with  $\hat{\alpha} = 5$ ; for the dotted and dash-dotted curves we use the  $\mathcal{L}^{(2)}$  amplitude plus that obtained from  $\mathcal{L}^{(4)}$  with  $L_{9L} = 5$  and  $L_{9R} = 5$  respectively.

Since  $L_{10}$  is proportional to the parameter  $\epsilon_3$  measured at LEP I, we have a very strong constraint on it. Including all the LEP results, as well as all the relevant low energy data, Altarelli finds  $\epsilon_3 = (3.5 \pm 2.8) \times 10^{-3}$  [6]. This corresponds to

$$L_{10}(M_Z) = -1.31 \pm 1.05. \quad (18)$$

Our calculation in this paper is at tree-level only, so it is not appropriate to include the running of  $L_{10}$ . That running, however, would be a very small effect [8]. Since the process  $e^- \gamma \rightarrow \nu W^- Z$  is only sensitive to much larger values of  $L_{10}$  than allowed by Eq. 18, we will not consider this operator in any detail.

We see that, as expected, the cross section is increasingly more sensitive to the anomalous couplings at higher energies. Our result confirms that the amplitude from the term with coupling  $\hat{\alpha}$  grows more rapidly with energy than the other terms. As we argued before, the parity violating nature of this operator allows it to generate a “maximally” enhanced amplitude growing as  $(s_{WZ})^{3/2}$ , whereas the amplitudes from the operators with the  $L_{9L}$ ,  $L_{9R}$  couplings only grow as  $s_{WZ}$  asymptotically. The relative sensitivity of this process to  $\hat{\alpha}$  is thus enhanced at high energies.

In accordance with the “naturalness” assumption that we have adopted, we compute the cross section numerically by looking at one anomalous coupling at a time, and further parameterize it as:

$$\sigma = \left( c_0 + c_1 L_i + c_2 L_i^2 \right) \text{ fb}, \quad (19)$$

where  $L_i$  generically represents an anomalous coupling constant. The first term,  $c_0$ , is the contribution from the lowest order Lagrangian, which is numerically equal to what would be found in the Standard Model at **tree** level. This is because the Higgs boson in the Standard Model does not enter the calculation of this process at tree level. The  $c_1$  term corresponds to the interference between the lowest order amplitude and the amplitude due to the coupling  $L_i$ . The  $c_2$  term is the contribution to the cross section from the square of the amplitude corresponding to the coupling  $L_i$ . Notice that since we only consider one anomalous coupling at a time, there is no interference between amplitudes corresponding to different anomalous couplings.

We first consider the case of an  $e^+e^-$  linear collider with  $\sqrt{s_{ee}} = 0.5$  TeV. This  $e^+e^-$  center of mass energy yields a spectrum for  $\sqrt{s_{e\gamma}}$  that peaks at about 0.45 TeV. The coefficients for Eq. 19 are presented in Table 1. To roughly simulate the detector performance, we have used the following minimal acceptance cuts,

$$|\cos \theta_V| < 0.9, \quad p_T(WZ) > 15 \text{ GeV}, \quad (20)$$

where the  $\theta_V$  cut is applied to both the polar angle of  $W$  and  $Z$ , and  $p_T(WZ)$  is the transverse momentum of the gauge-boson pair. This cut insures that there is sufficient missing energy in the event to suppress possible backgrounds. A more detailed discussion of reducible backgrounds will be deferred to the end of this section. For each coefficient, the first row in the table corresponds to the numbers obtained without cuts and the second row gives the results with the cuts. The constant  $c_0$ , which gives the minimal SM rate, is found at  $\sqrt{s_{ee}} = 0.5$  TeV to be:

$$c_0 = \begin{cases} 69.3 & \text{no cuts} \\ 42.9 & \text{with cuts.} \end{cases}$$

Table 1: Coefficients in Eq. 19 for  $\sqrt{s_{ee}} = 0.5$  TeV. Cuts are given in Eq. 20

	$\hat{\alpha}$	$L_{9L}$	$L_{9R}$	$L_{9L} = L_{9R}$	$L_{10}$
$c_1$	0.324	0.746	0.281	1.03	0.312
$c_1$ with cuts	0.209	0.444	0.169	0.613	0.187
$c_2$	$3.80 \times 10^{-2}$	$4.30 \times 10^{-3}$	$7.60 \times 10^{-4}$	$7.33 \times 10^{-3}$	$2.99 \times 10^{-3}$
$c_2$ with cuts	$2.81 \times 10^{-2}$	$2.58 \times 10^{-3}$	$5.22 \times 10^{-4}$	$4.63 \times 10^{-3}$	$1.99 \times 10^{-3}$

Although the dynamical distributions with anomalous couplings are not significantly different from those of the SM at  $\sqrt{s_{ee}} = 0.5$  TeV, one can try to measure deviations from the SM results based on the total event rate by computing the statistical significance, which is taken as

$$S = \frac{\text{signal events}}{\sqrt{\text{background events}}}. \quad (21)$$

In our case, the “signal” events correspond to the second and third terms in Eq. 19, and the “background” events to the minimal SM rate (the first term in Eq. 19). A  $3\sigma$  significance resulting from the anomalous couplings is given in Fig. 3 for  $\hat{\alpha}$ ,  $L_{9L}$ ,  $L_{9R}$ , and  $L_{9L} = L_{9R}$ , respectively, versus the integrated luminosity at  $\sqrt{s_{ee}} = 0.5$  TeV. There is comparable sensitivity to  $\hat{\alpha}$  and  $L_{9L}$ , and it seems quite feasible for an  $e^+e^-$  machine with  $\sqrt{s_{ee}} = 0.5$  TeV running in the  $e\gamma$  mode, to reach a sensitivity of order of  $10 (\Lambda/2 \text{ TeV})^2$  to these couplings with an integrated luminosity of  $10 - 20 \text{ fb}^{-1}$ . Such a machine is significantly less sensitive to  $L_{9R}$ , however.

To demonstrate the significant increase in sensitivity to  $\hat{\alpha}$  at higher energies, we now consider a 2 TeV  $e^+e^-$  collider. As we have discussed before, we expect the amplitude proportional to  $\hat{\alpha}$  to grow faster with energy than the other amplitudes. This feature is clearly demonstrated in Fig. 4(a), where the invariant mass distribution of the gauge boson pairs  $M(WZ)$  is shown at  $\sqrt{s_{ee}} = 2$  TeV for  $\hat{\alpha} = 3 (\Lambda/2 \text{ TeV})^2$  and  $L_{9L} = 10 (\Lambda/2 \text{ TeV})^2$ . The result for  $L_{9R}$  is similar to that for  $L_{9L}$  and is not shown here. We see the increasing importance of the  $\hat{\alpha}$  contribution as  $M(WZ)$  increases. The effect of the contribution from the  $L_9$  term is mostly to change the overall normalization. Figure 4(b) shows the  $\cos\theta_W$  distribution at  $\sqrt{s_{ee}} = 2$  TeV,

where  $\theta_W$  is the polar angle of the  $W$ -boson with respect to the  $e^-$  beam direction. The SM curve peaks sharply at  $\cos\theta_W = -1$ , this is due to the emission of the  $W$ -boson from the photon leg. The  $\hat{\alpha}$  anomalous interaction produces the  $W$ -boson more in the central region. We thus find that the contribution of  $L_9$  to the central region is relatively less important than that of  $\hat{\alpha}$ .

Since the effect of the  $L_9$  interactions is mainly an overall normalization, to maintain a high sensitivity to the  $L_9$  coefficients we take moderate acceptance cuts which will retain most of the signal:

$$|\cos\theta_V| < 0.9, \quad p_T(WZ) > 30 \text{ GeV}. \quad (22)$$

Here the  $p_T(WZ)$  cut is optimized to suppress reducible backgrounds from other sources. On the other hand, the results in Fig. 4 imply the possibility of improving the sensitivity to  $\hat{\alpha}$  by a set of more stringent cuts:

$$|\cos\theta_V| < 0.8, \quad p_T(WZ) > 30 \text{ GeV}, \quad M(WZ) > 0.5 \text{ TeV}. \quad (23)$$

The coefficients of Eq. 19 for  $\sqrt{s_{ee}} = 2 \text{ TeV}$  are given in Table 2. Again, the first row corresponds to the case with no cuts, the second row presents numbers with the cuts of Eq. 22, and the third row shows the numbers with the cuts of Eq. 23. The minimal SM rates are

$$c_0 = \begin{cases} 936 & \text{no cuts} \\ 209 & \text{with cuts Eq. 22} \\ 38.8 & \text{with cuts Eq. 23} \end{cases}.$$

Table 2: Coefficients in Eq. 19 for  $\sqrt{s_{ee}} = 2 \text{ TeV}$ . Cuts are given in Eqs. 22 and 23

	$\hat{\alpha}$	$L_{9L}$	$L_{9R}$	$L_{9L} = L_{9R}$	$L_{10}$
$c_1$	1.03	10.0	3.46	13.5	4.79
$c_1$ with cuts Eq. (22)	0.331	1.97	0.712	2.68	1.03
$c_1$ with cuts Eq. (23)	0.144	0.393	0.121	0.515	0.225
$c_2$	9.22	0.165	0.0425	0.294	0.195
$c_2$ with cuts Eq. (22)	6.13	0.0565	0.028	0.137	0.122
$c_2$ with cuts Eq. (23)	5.12	0.0282	0.0187	0.0820	0.0791

At  $\sqrt{s_{ee}} = 2 \text{ TeV}$ , we find that the contribution linear in  $\hat{\alpha}$  has a much smaller coefficient than the quadratic term. This is consistent with the fact that within the effective  $W$  approximation, this interference term vanishes [11]. In the full calculation it is suppressed by  $M_W^2/s_{WZ}$  with respect to the quadratic term. This effect is not so apparent at the lower energy,  $\sqrt{s_{ee}} = 0.5 \text{ TeV}$ . At  $\sqrt{s_{ee}} = 2 \text{ TeV}$ , our results agree well with those obtained using the effective  $W$  approximation.

A  $3\sigma$  significance resulting from the anomalous couplings  $\hat{\alpha}$ ,  $L_{9L}$ , and  $L_{9R}$ , respectively at  $\sqrt{s_{ee}} = 2 \text{ TeV}$  is given in Figs. 5 and 6 for the cuts of Eq. 22 and Eq. 23, as a

function of the integrated luminosity. The curves in (a) correspond to positive values of the anomalous couplings, while those in (b) to negative values. It is seen that the negative values are always more difficult to probe. In Fig. 5(b), the solid curve for  $\hat{\alpha}$  and the dotted curve on the top for  $-L_{9L} = -L_{9R}$  are for  $+3\sigma$  effects as are those in Fig. 5(a). There are also three contour-like curves labelled by  $-3\sigma$ , which reflect the fact that  $c_1 L_i + c_2 L_i^2 < 0$  in Eq. 19. This indicates that for certain negative values of the  $L_i$ , there are significant cancellations between the linear and quadratic terms. However, with the more stringent cuts of Eq. 23, we see from Fig. 6(b) that this effect disappears. We therefore consider the cancellation to be an accident. From Fig. 5, we find that the process  $e\gamma \rightarrow \nu WZ$  could probe  $L_9$ 's at a level of  $2 - 5 (\Lambda/2 \text{ TeV})^2$  with an integrated luminosity of about  $100 \text{ fb}^{-1}$  and that it is more sensitive to  $\hat{\alpha}$ . The cuts of Eq. 23 are effective in suppressing the lowest order contribution (SM), which is roughly reduced by a factor of 25 while the coefficient  $c_2$  for the  $\hat{\alpha}$  amplitude is reduced by less than a factor of 2. We see from Fig. 6 that the coefficient  $\hat{\alpha}$  can be probed here to a level less than  $1 (\Lambda/2 \text{ TeV})^2$ .

So far we have based our discussion on the excess of events above the SM prediction. Without distinctive features in some dynamical distribution, it might be hard to convincingly establish a signal for new physics. Given the parity violating nature of the operator multiplying  $\hat{\alpha}$  we might try to enhance the sensitivity to this coupling by studying a parity odd observable, such as a correlation  $\vec{p}_e \cdot (\vec{p}_W \times \vec{p}_Z)$ . Notice, however, that there is no reason for this correlation to vanish in the minimal SM where parity is violated maximally. As a measure of the size of this correlation we can construct an associated forward-backward asymmetry. We find that for a 500 GeV collider the interference term between  $\hat{\alpha}$  and the lowest order amplitude can contain an asymmetry of order 10% for a right-handed photon. The choice of a right-handed photon is motivated by the fact that this polarization enhances the relative size of the  $\hat{\alpha}$  term in the total cross-section in the effective  $W$  approximation [11]. However, since this interference term is much smaller than the lowest order term, the measurable asymmetry gets diluted to a negligible level. Since the relative importance of the interference between the lowest order amplitude and the amplitude proportional to  $\hat{\alpha}$  decreases as the center of mass energy increases, and since a correlation of the type  $\vec{p}_e \cdot (\vec{p}_W \times \vec{p}_Z)$  appears in this interference, we expect the asymmetry to be even smaller in a 2 TeV collider. Even though it is very difficult to single out the  $\hat{\alpha}$  term with a parity odd observable, we can still study this contribution at high energies. As we discussed earlier, the existence of  $\hat{\alpha}$  significantly enhances the cross section in the high  $M(WZ)$  and central region, making the separation of the  $\hat{\alpha}$  contribution feasible, as can be seen from Fig. 4. Due to a Jacobian peak in the  $WZ$  two-body kinematics, similar enhancements in the  $p_T(W)$  or  $p_T(Z)$  distributions also appear in the high energy region.

The existing data from the CERN  $p\bar{p}$  collider [16] and LEP I [17] only constrain the anomalous couplings  $L_{9R,9L}$  rather weakly. The bound is  $|\Delta\kappa| \simeq 1 - 2$ , which translates into  $L_{9R,9L} < (300 - 600) (\Lambda/2 \text{ TeV})^2$ . The Fermilab Tevatron with an integrated luminosity of  $100 \text{ fb}^{-1}$  can provide comparable results to this bound [18].

Ref. [9] finds that the LHC will be sensitive to values  $L_{9R} > 61 (\Lambda/2 \text{ TeV})^2$  and  $L_{9R} < -63 (\Lambda/2 \text{ TeV})^2$ ;  $L_{9L} > 5 (\Lambda/2 \text{ TeV})^2$  and  $L_{9L} < -9 (\Lambda/2 \text{ TeV})^2$ . It is well known that LEP II will provide a good environment to study the three gauge-boson anomalous couplings [19] at a sensitivity of  $|\Delta\kappa| \simeq 4 \times 10^{-2}$ . This corresponds to  $L_{9R,9L} \simeq 12 (\Lambda/2 \text{ TeV})^2$ . There are several studies in the literature for an  $e^+e^-$  machine with  $\sqrt{s_{ee}} = 0.5 \text{ TeV}$  concentrating on the  $e^+e^- \rightarrow W^+W^-$  mode. The claim is that a sensitivity of order  $5 \times 10^{-3}$  to  $\Delta\kappa_\gamma$  can be reached with  $50 \text{ fb}^{-1}$  integrated luminosity [20]. This would correspond to potential sensitivities of about  $(1 - 2) (\Lambda/2 \text{ TeV})^2$  to the couplings  $L_{9L}$ ,  $L_{9R}$ , and  $L_{10}$  (we have made no attempt to study differences between these three couplings in that process). This machine running in the  $e\gamma$  mode is also considered in Ref. [21] as a means of searching for anomalous couplings, and it is found that with  $50 \text{ fb}^{-1}$  a 7% sensitivity to  $\Delta\kappa$ , corresponding to  $L_{9R,9L} \sim 20$ , is feasible. In contrast, not many studies have been done in the literature concerning the coupling  $g_5$  (or  $\hat{\alpha}$ ). It was found in Ref. [11] that the process  $e^+e^- \rightarrow W^+W^-$  may be sensitive to  $g_5$  at a high energy  $e^+e^-$  machine if highly polarized electron beams can be obtained.

Finally, let us comment on the event reconstruction and other possible backgrounds. With the leptonic decays of  $W \rightarrow l\nu$ ,  $Z \rightarrow l\bar{l}$ , there is little background to anomalous coupling signals except for the lowest order  $WZ$  production which we have systematically included in our discussion ( $c_0$  in Eq. 19). In estimating the sensitivities in our figures, we have implicitly assumed the full use of the hadronic decay modes, in which the four jets in pairs reconstruct to  $M_W$  and  $M_Z$ . The inclusion of the hadronic modes increases the event rate significantly and will make a better  $M(WZ)$  mass reconstruction possible as well. It would be ideal to have a good hadronic energy resolution (better than  $M_Z - M_W \sim 10 \text{ GeV}$ ) in order to be able to distinguish the  $W$  or  $Z$  decays via the di-jet mass. If possible, this would essentially eliminate other backgrounds. Given the fact that this hadronic energy resolution may be difficult to achieve, one has to make use of other kinematic cuts to reduce potential backgrounds. The potential backgrounds are  $e^-\gamma \rightarrow W^+W^-e^-$ ,  $ZZe^-$ ,  $b\bar{t}\nu$ , and  $t\bar{t}e^-$ , which have all been analysed in Ref. [3] in the search for the SM Higgs boson. Among the backgrounds, the  $ZZe^-$ ,  $b\bar{t}\nu$ , and  $t\bar{t}e^-$  are at least an order of magnitude smaller than the SM process  $e^-\gamma \rightarrow W^-Z\nu$  and they are sufficiently different from our signal process in terms of the final state particles and kinematics. However, the cross section for the process  $e^-\gamma \rightarrow W^+W^-e^-$  is about an order of magnitude larger than the SM  $WZ$  process. Based on the fact that the major contribution to  $e^-\gamma \rightarrow W^+W^-e^-$  is from the almost on-shell photon exchange  $\gamma\gamma \rightarrow W^+W^-$ , we can substantially reduce it by pushing the photon propagator away from the pole. Our  $p_T(WZ)$  cut is designed for this purpose. Furthermore, in our  $WZ$  signal the transverse momentum of the boson pair is balanced by the missing transverse momentum (essentially from the  $\nu$ ); whereas the  $e^-\gamma \rightarrow W^+W^-e^-$  background will have a visible  $e^-$  with large transverse momentum. We can therefore further reduce this background by requiring not only large  $p_T(WZ)$  but also, at the same, time vetoing the hard electrons [3]. Overall, the only significant irreducible background for our study of anomalous couplings is the

lowest order SM process  $e^-\gamma \rightarrow W^-Z\nu$ , which we have included.

## 4 Conclusions

If the electroweak symmetry breaking sector is strongly coupled, and no light resonances are found, then one expects deviations of the gauge-boson self-interactions from the SM predictions. An  $e\gamma$  collider operating at  $\sqrt{s_{ee}} > 0.5$  TeV can provide important input into our understanding of the nature of electroweak symmetry breaking. Such a collider would provide more precise measurements of  $L_{9L,9R}$  than the LHC via the process  $e^-\gamma \rightarrow \nu W^-Z$ . Due to the gauge structure and the relatively large contribution of the gauge-boson self-interactions to this process, it is as useful in studying anomalous couplings as the lower order process  $e^-\gamma \rightarrow \nu W^-$  [21]. Although the process  $e^+e^- \rightarrow W^+W^-$  is better to study the coefficients  $L_{9L,9R}$ , the process  $e^-\gamma \rightarrow \nu W^-Z$  is very sensitive to the coupling  $\hat{\alpha}$ , especially at higher energies. We find that an  $e^+e^-$  machine operating in the  $e\gamma$  mode with  $\sqrt{s_{ee}} = 0.5$  TeV can place bounds of order  $\hat{\alpha} < 10 (\Lambda/2 \text{ TeV})^2$  with  $20 \text{ fb}^{-1}$  integrated luminosity. Similarly, it is possible at a 2 TeV  $e^+e^-$  collider running in the  $e\gamma$  mode to place the bound  $\hat{\alpha} < .6 (\Lambda/2 \text{ TeV})^2$ , which corresponds to  $g_5^Z < 5 \times 10^{-3} (\Lambda/2 \text{ TeV})^2$ . Observation of enhanced production of longitudinal  $WZ$  pairs in the high  $M(WZ)$  region and at central  $\cos\theta_W$  could be a direct indication for a new interaction of the form proportional to  $\hat{\alpha}$ .

## Acknowledgments

The work of S. Dawson is supported by the U.S. DOE under contract DE-AC02-76CH00016. K.C. is supported by the U.S. DOE grant DE-FG02-91-ER40684. T.H. is supported in part by the DOE grant DE-FG03-91ER40674 and in part by a UC-Davis Faculty Research Grant.

## A Feynman Rules

The three gauge boson vertex in unitary gauge for  $Z^\sigma(k) \rightarrow W^{+\mu}(p^+) + W^{-\nu}(p^-)$  can be written

$$iC_Z^{\mu\nu\sigma}(p^+, p^-, k) \equiv ie_* \frac{c_Z}{s_Z} \left\{ \left[ (p^+ - p^-)^\sigma g^{\mu\nu} + 2p^{-\mu} g^{\nu\sigma} - 2p^{+\nu} g^{\mu\sigma} \right] g_1^Z + \left[ k^\mu g^{\nu\sigma} - k^\nu g^{\mu\sigma} \right] \kappa_Z + ig_5^Z \epsilon^{\mu\sigma\nu\rho} (p^+ - p^-)^\rho \right\} . \quad (24)$$

The momentum is defined such that  $k$  is incoming and  $p^+, p^-$  are outgoing.

Similarly the three gauge boson vertex in unitary gauge for  $\gamma^\sigma(k) \rightarrow W^{+\mu}(p^+) + W^{-\nu}(p^-)$  can be written

$$iC_\gamma^{\mu\nu\sigma}(p^+, p^-, k) \equiv ie_* \left\{ \left[ (p^+ - p^-)^\sigma g^{\mu\nu} + 2p^{-\mu} g^{\nu\sigma} - 2p^{+\nu} g^{\mu\sigma} \right] g_1^\gamma \right.$$

$$+ \left[ k^\mu g^{\nu\sigma} - k^\nu g^{\mu\sigma} \right] \kappa_\gamma \} \quad (25)$$

The four gauge boson vertex in unitary gauge for  $W_\mu^+ W_\nu^- \gamma_\kappa Z_\lambda$  is,

$$i\tilde{C}_{WWZA}^{\mu\nu\kappa\lambda} = -ie_*^2 \frac{c_Z}{s_Z} \left\{ \left[ 2g_{\kappa\lambda}g_{\mu\nu} - g_{\kappa\mu}g_{\lambda\nu} - g_{\kappa\nu}g_{\lambda\mu} \right] g_1^Z - 2ig_5^Z \epsilon^{\nu\mu\lambda\kappa} \right\} \quad , \quad (26)$$

where all particles are incoming.

The renormalization of the couplings given in Eq. 7 also affects the fermion- gauge boson vertices. For  $e^+ \nu \rightarrow W_\mu^+$  we find:

$$i\Gamma^\mu = -i \frac{e_*}{2\sqrt{2}s_Z} \left[ 1 - \frac{e_*^2}{s_Z^2 - c_Z^2} L_{10} \frac{v^2}{\Lambda^2} \right] \gamma_\mu (1 - \gamma_5) \quad . \quad (27)$$

For a fermion with charge  $eQ_f$  and isospin  $T_{3f} = \pm 1$ , the  $\bar{f}f \rightarrow Z_\mu$  coupling is:

$$i\tilde{\Gamma}_\mu = -i \frac{e_*}{4s_Z c_Z} \gamma_\mu \left[ R_e (1 + \gamma_5) + L_e (1 - \gamma_5) \right] \quad (28)$$

where

$$\begin{aligned} R_f &= -2Q_f \left[ s_Z^2 - \frac{e_*^2}{c_Z^2 - s_Z^2} L_{10} \frac{v^2}{\Lambda^2} \right] \\ L_f &= R_f + T_{3f} \quad . \end{aligned} \quad (29)$$

The  $\bar{f}fA$  vertices have the same form as they do in the minimal standard model but they are now given in terms of  $e_*$ .

## References

- [1] I. F. Ginzburg *et. al.*, *Nucl. Phys.* **B228** 285 (1983); I. F. Ginzburg *et. al.*, *Nucl. Instrum. & Methods* **205** 47 (1983); *ibid* **219** 5 (1984); V. I. Telnov, *Nucl. Instrum. & Methods* **A294** 72 (1990); D. Bauer, D. Borden, D. Miller, and J. Spence, *9th International Workshop on Photon-Photon Collisions*, San Diego, CA. 1992; .
- [2] Kingman Cheung, *Nucl. Phys.* **B403** 572 (1993); S. Moretti, DFTT 79/93.
- [3] Kingman Cheung, *Phys. Rev.* **D48** 1035 (1993).
- [4] S. Godfrey, G. Couture, and P. Kalyniak, *Beyond the Standard Model*, Ames, Iowa, 1988; S. Godfrey, G. Couture, and P. Kalyniak, *11th Annual Montreal-Rochester-Syracuse-Toronto Meeting*, Syracuse, N.Y., 1989; E. Yehudai, *Phys. Rev.* **D41** 33 (1990); G. Couture, S. Godfrey, P. Kalyniak, *Phys. Lett.* **218B** 361 (1989); G. Belanger and F. Boudjema, *Phys. Lett.* **288B** 201 (1992); D. Espriu and M. Herrero, *Nucl. Phys.* **B373** 117 (1992); A. Dobado and J. Urdiales, *Phys. Lett.* **292B** 129 (1992); R. Casalbuoni *et. al.*, *Nucl. Phys.* **B409** 257 (1993); D. Choudhury and F. Cuyper, MPI-Ph/93-98 .

- [5] T. Appelquist and C. Bernard, *Phys. Rev.* **D22** 200 (1980); A. Longhitano, *Nucl. Phys.* **B188** 118 (1981).
- [6] G. Altarelli, Plenary Talk given at the EPS Conference on High Energy Physics, Marseille, France, July 1993, CERN-TH-7045/93.
- [7] B. Holdom, *Phys. Lett.* **258B** 156 (1991).
- [8] J. Bagger, S. Dawson and G. Valencia, *Nucl. Phys.* **B399** 364 (1993).
- [9] A. Falk, M. Luke, and E. Simmons, *Nucl. Phys.* **B365** 523 (1991).
- [10] T. Appelquist and G.-H. Wu, *Phys. Rev.* **D48** 3235 (1993).
- [11] S. Dawson and G. Valencia, *Phys. Rev.* **D49** 2188 (1994).
- [12] D. Kennedy and B. Lynn, *Nucl. Phys.* **B322** 1 (1989).
- [13] K. Hagiwara *et al.*, *Nucl. Phys.* **B282** 253 (1987).
- [14] F. Boudjema, *Proceedings of Physics and Experiments with Linear  $e^+e^-$  Colliders*, ed. by F. A. Harris *et al.*, (1993), p. 713, and references therein.
- [15] O. Eboli, M. Gonzalez-Garcia, and S. Novaes, MAD-PH-764, (1993).
- [16] UA2 Collaboration, J. Alitti *et al.*, *Phys. Lett.* **277B** 194 (1992).
- [17] K. Hagiwara *et al.*, *Phys. Rev.* **D48** 2182 (1993).
- [18] U. Baur and E. L. Berger, *Phys. Rev.* **D41** 1476 (1990); U. Baur, T. Han, and J. Ohnemus, *Phys. Rev.* **D48** 5140 (1993).
- [19] M. Kuroda, F. M. Renard, and D. Schildknecht, *Phys. Lett.* **183B** 366 (1987).
- [20] For a review, see, *e. g.*, A. Miyamoto, in *Proceedings of Physics and Experiments with Linear  $e^+e^-$  Colliders*, ed. by F. A. Harris *et al.*, (1993), p. 141, and references therein.
- [21] S. Godfrey and K. A. Peterson, in *Proceedings of Physics and Experiments with Linear  $e^+e^-$  Colliders*, ed. by F. A. Harris *et al.*, (1993), p. 731.



## FIGURE CAPTIONS

1. Diagrams contributing to the process  $e^-\gamma \rightarrow \nu W^- Z$ . The dashed circle represents three and four gauge boson couplings arising from  $\mathcal{L}^{(2)} + \mathcal{L}^{(4)}$  as given in the appendix. The full circle represents the renormalized fermion-gauge-boson coupling as given in the appendix.
2. Total cross section for  $e^+e^- \rightarrow e^+\nu W^- Z$  (in the  $e^-\gamma$  mode) as a function of  $\sqrt{s_{ee}}$ . The solid curve is the result of the lowest order effective Lagrangian. To this lowest order result, we have added the contributions from non-zero couplings with  $\Lambda = 2$  TeV: The dashed line corresponds to  $\hat{\alpha} = 5$  and the dotted and dashed lines correspond to  $L_{9L}, L_{9R} = 5$ , respectively. The effect of  $L_{10}$  subject to the constraint of Eq. 18 is so small that it cannot be distinguished from the lowest order SM result.
3.  $3\sigma$  sensitivity of an  $e^+e^-$  collider at  $\sqrt{s_{ee}} = 0.5$  TeV (operating in the  $e^-\gamma$  mode) to  $\hat{\alpha}, L_{9L}$  and  $L_{9R}$  with the cuts Eq. 20. The curves are shown as a function of integrated luminosity. We set  $\Lambda = 2$  TeV.
4. Differential cross sections (a)  $d\sigma/dM(WZ)$  and (b)  $d\sigma/d(\cos\theta_W)$  for  $e^+e^- \rightarrow e^+\nu W^- Z$ .  $\theta_W$  is the polar angle between the  $W^-$  and the  $e^-$  in the lab frame and the total center of mass energy  $\sqrt{s_{ee}} = 2$  TeV. The curves show the result for the lowest order effective Lagrangian (solid, labeled as SM), for  $\hat{\alpha} = 3$  (dashes), and for  $L_{9L}$  (dots) respectively, for  $\Lambda = 2$  TeV.
5. Same as Figure 3 but for  $\sqrt{s_{ee}} = 2$  TeV with the set of cuts Eq. 22. (a) for positive values of anomalous couplings and (b) for negative.
6. Same as Figure 3 but for  $\sqrt{s_{ee}} = 2$  TeV with the set of cuts Eq. 23. (a) for positive values of anomalous couplings and (b) for negative.

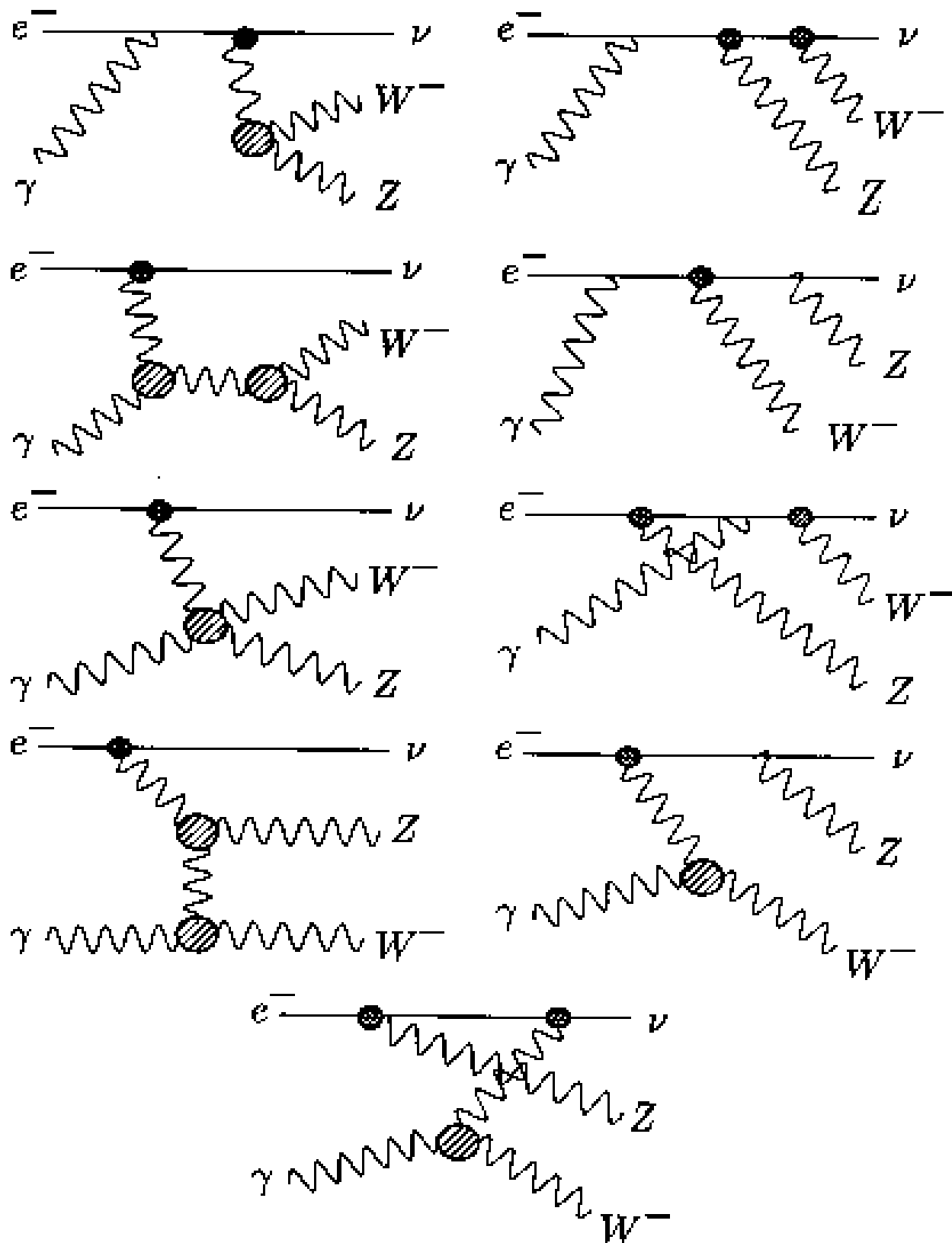


Figure 1

This figure "fig1-1.png" is available in "png" format from:

<http://arXiv.org/ps/hep-ph/9403358v1>

This figure "fig1-2.png" is available in "png" format from:

<http://arXiv.org/ps/hep-ph/9403358v1>

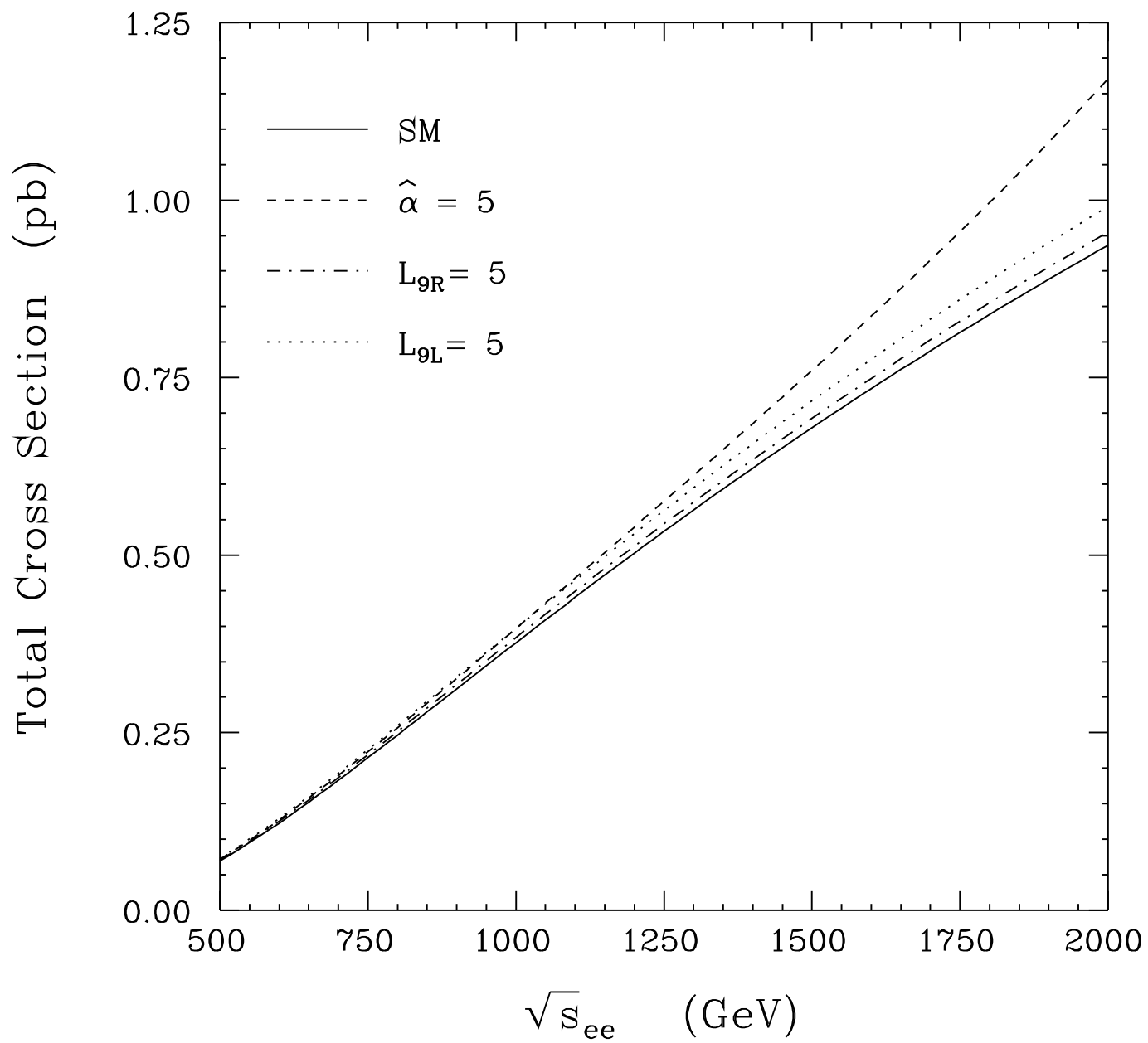


Fig. 2

This figure "fig1-3.png" is available in "png" format from:

<http://arXiv.org/ps/hep-ph/9403358v1>

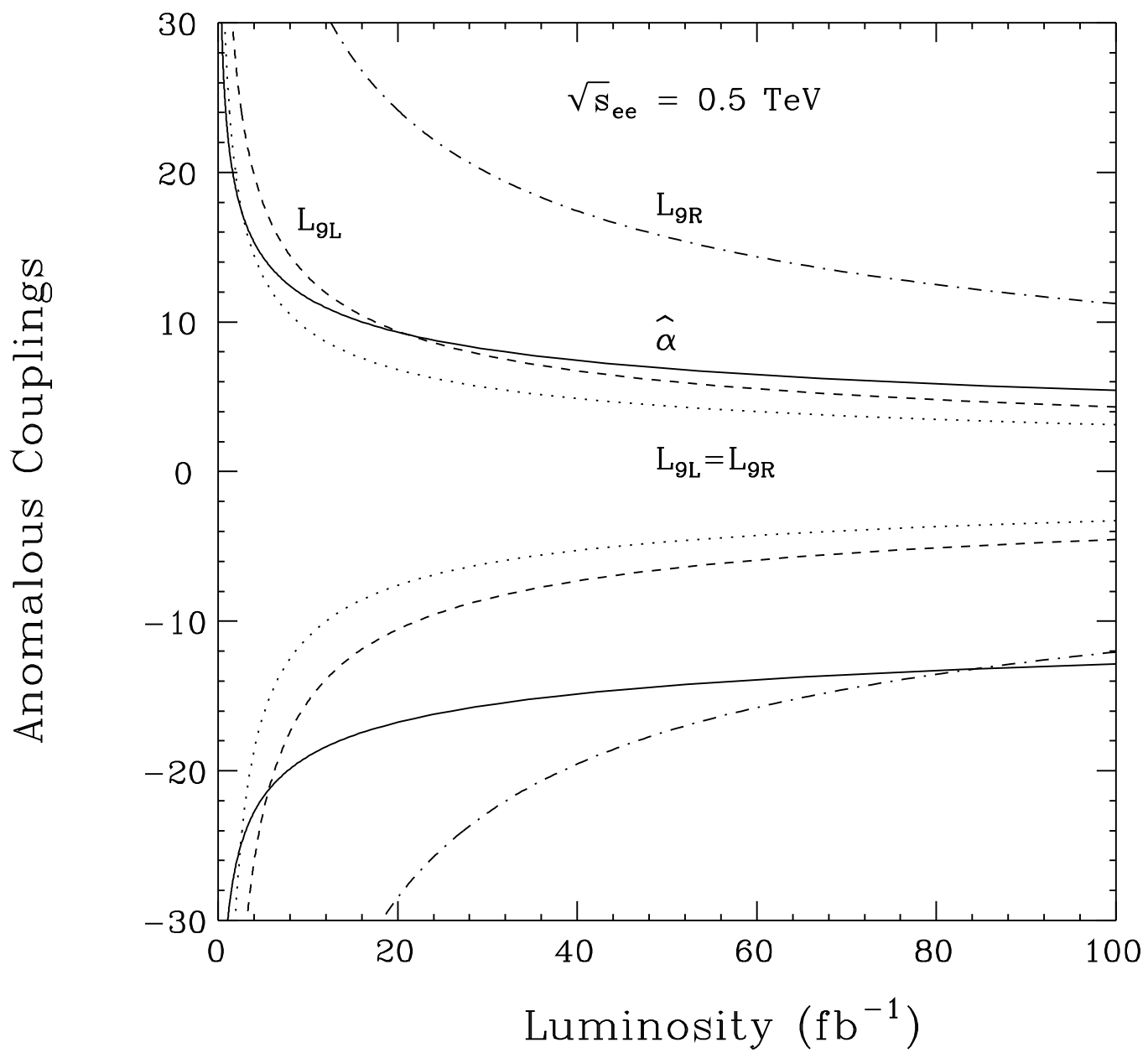


Fig. 3

This figure "fig1-4.png" is available in "png" format from:

<http://arXiv.org/ps/hep-ph/9403358v1>



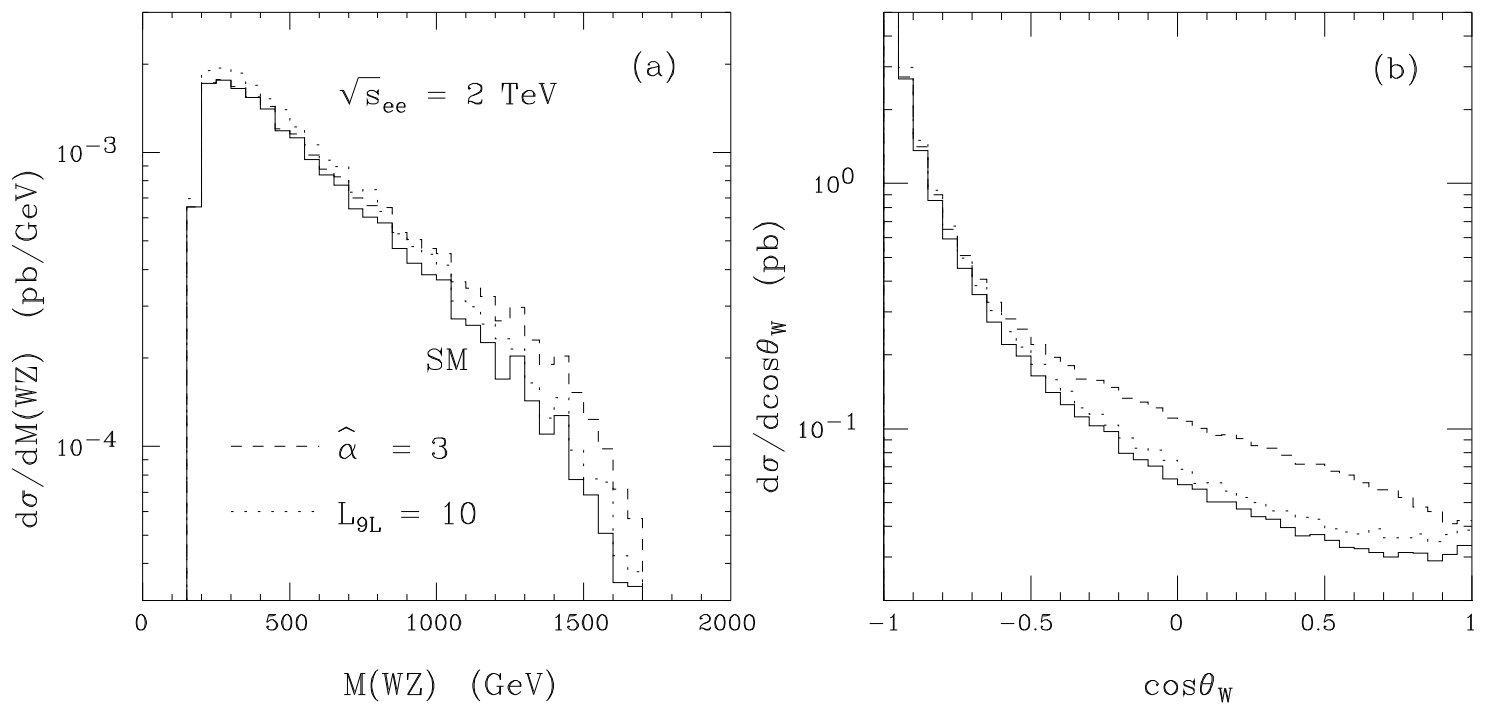


Fig. 4

This figure "fig1-5.png" is available in "png" format from:

<http://arXiv.org/ps/hep-ph/9403358v1>

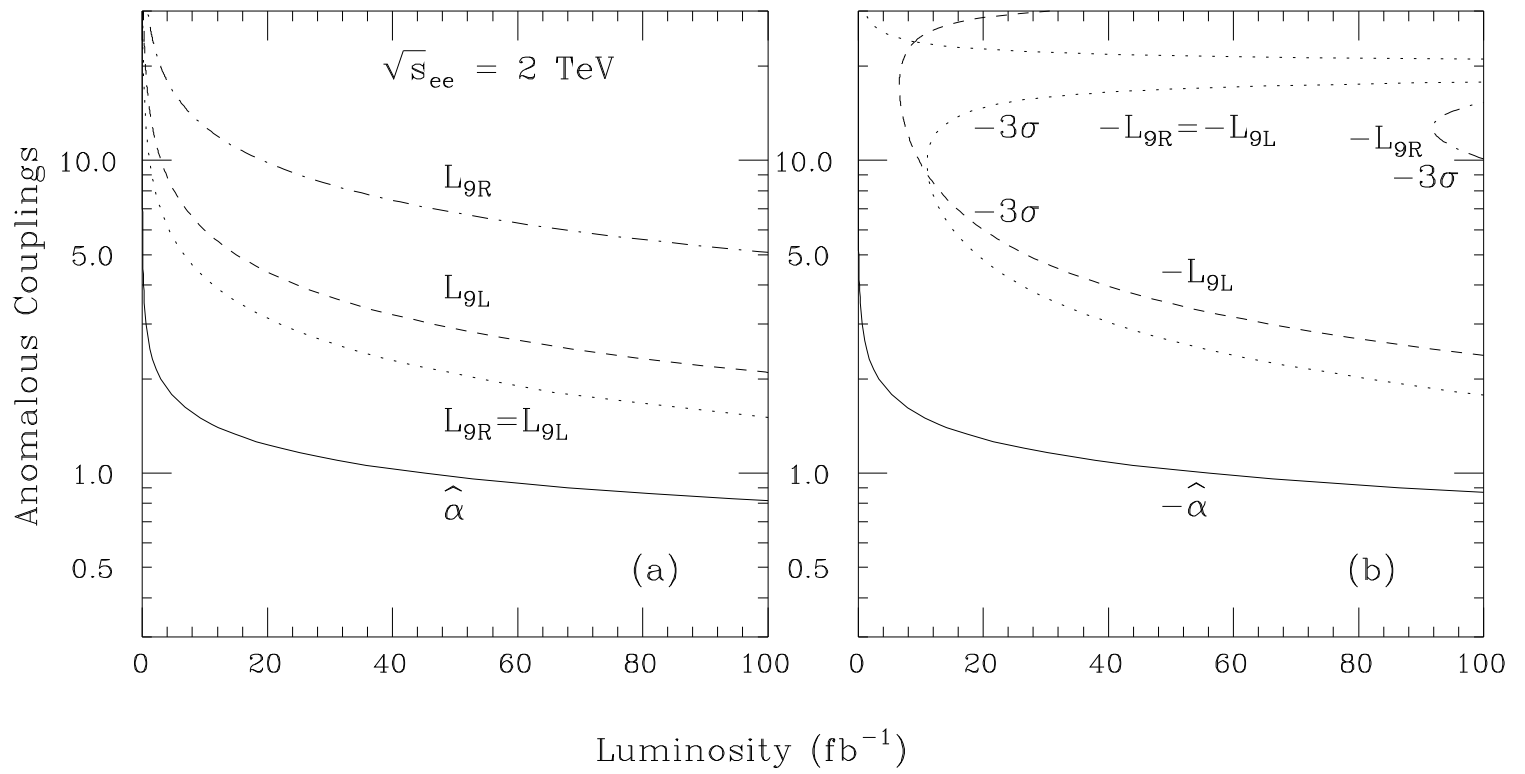


Fig. 5

This figure "fig1-6.png" is available in "png" format from:

<http://arXiv.org/ps/hep-ph/9403358v1>

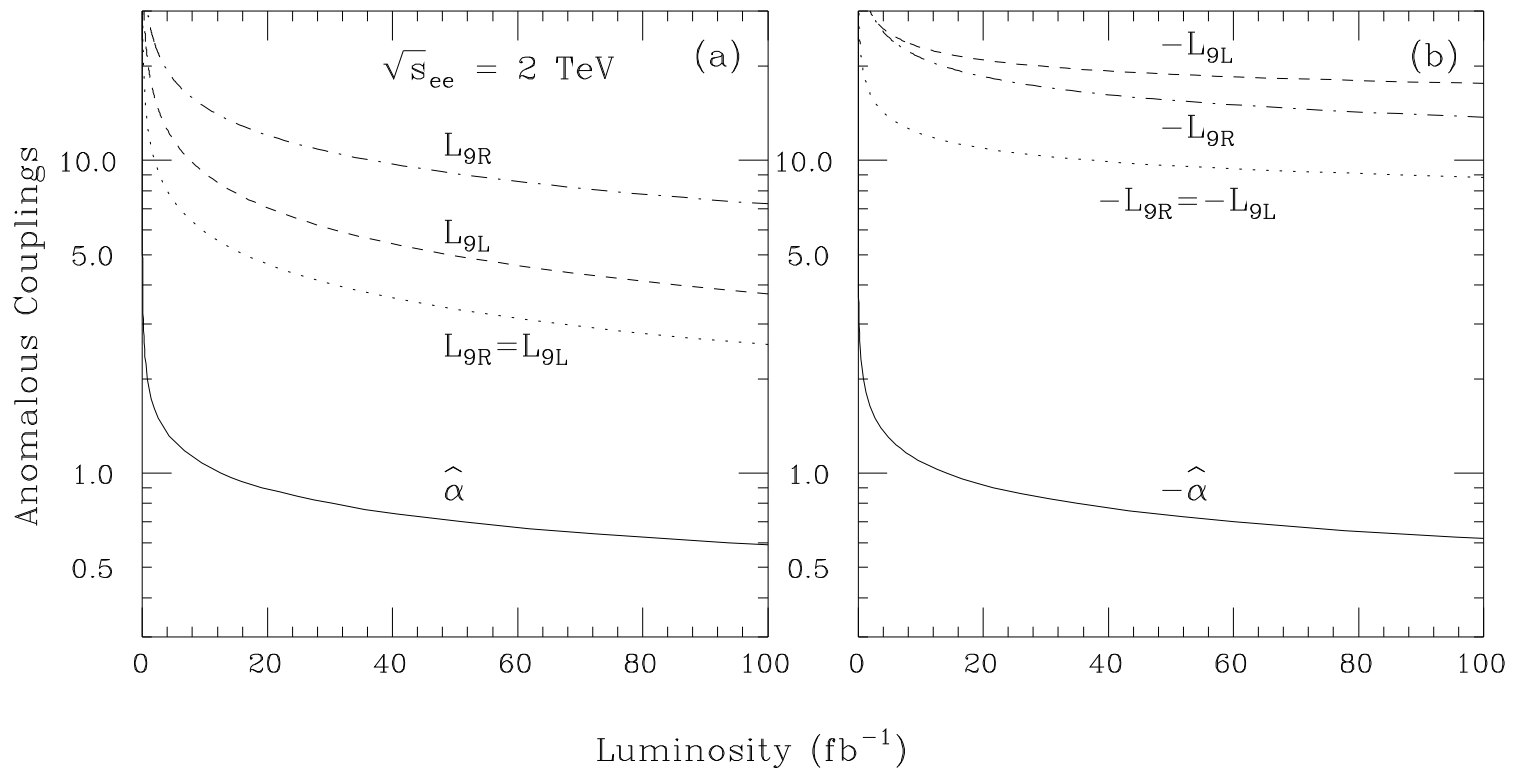


Fig. 6